Mass-Analyzed Threshold Ionization Spectroscopy of the Selected Rotamers of Hydroquinone and *p*-Dimethoxybenzene Cations

J. L. Lin, L. C. L. Huang, and W. B. Tzeng*

Institute of Atomic and Molecular Sciences, Academia Sinica, P.O. Box 23-166, 1 Section 4, Roosevelt Road, Taipei 106, Taiwan, Republic of China

Received: June 19, 2001

Mass-analyzed threshold ionization (MATI) spectroscopy in conjunction with two-color resonant two-photon excitation was used to investigate the ionic properties of the selected rotamers of hydroquinone (HYQ) and *p*-dimethoxybenzene (PDMB). The observed lower adiabatic ionization energy for the trans conformer is in good agreement with that predicted by ab initio and density functional calculations. With the exception of mode 6a of PDMB, the frequencies of the observed cation vibrations are close to each other for the two rotamers. Detailed analyses on the atomic displacement based on ab initio calculations show that the vibrational frequency of each mode can reflect the extent of the OH and OCH_3 substitutents' involvement in the overall molecular motions. The present experiments also demonstrate that a particular conformer can be selected from a chemical sample for recording the vibrational spectra of the cations. In principle, this method can be used not only for species identification but also for separation of molecular conformers.

1. Introduction

It is known that molecules with the same mass may have several stable structural isomers, which possess diverse reactivity in biochemical processes.[1,2] For example, there are three isomers of dihydroxybenzene: catechol (1,2-dihydroxybenzene), resorcinol (1,3-dihydroxybenzene), and hydroquinone (1,4-dihydroxybenzene). Some of these structural isomers may have different rotational conformers, which have different photochemical properties. Since these rotamers may coexist in a chemical sample, the identification and isolation of a particular species can be quite challenging. The laser spectroscopic methods in conjunction with a supersonic expansion technique can be used to yield discrete spectral features.[3,4] Since the origins of the electronic transitions of the various conformers may differ by only a few tens to a few hundreds of wavenumbers, the resulting vibronic features of the isomeric species may overlap in a common spectral region.[5] The confirmation of the existence of conformers generally requires other complimentary methods in addition to the typical laser induced fluorescence (LIF) or resonance-enhanced multiphoton ionization (REMPI) approaches.

It has been demonstrated that the combined REMPI, spectral hole-burning experimental data and ab initio calculations can give a persuasive conclusion for the existence of the rotamers.[6−9] The results show that only one conformer of catechol is dominant whereas two isomers of resorcinol contribute to the recorded spectra under molecular beam conditions. In addition, these methods also offer information about the structures and vibrations of molecular species in the S_0 and S_1 states. Gerhards, et al. have applied mass analyzed threshold ionization (MATI) spectroscopy to record the vibrational spectra of the three structural isomers of dihydroxybenzene.[10,11] The experimental results were satisfactorily supported by the density functional theory (DFT) and complete active space self-consistent field (CASSCF) calculations. They have concluded that there is only one stable structure of the catechol cation. However, there are two rotational isomers each for the resorcinol and hydroquinone cations.

The structure and vibrations of the rotamers of hydroquinone (HYQ) and *p*-dimethoxybenzene (PDMB) in the ground and lowest electronically excited states have been extensively investigated.[8−9,12−15] The results show that the planar cis and trans forms (hereafter, it is assumed that the methyl groups in PDMB are points for discussion throughout this paper) of these two molecules coexist in the S_0 and S_1 states. The argument for the coexistence of the two conformers is on account of (1) the observation of two series of bands in the vibronic spectra, (2) the experimental results from one-photon resonant two-photon and two-photon resonant four-photon laser spectroscopy, (3) the findings from hole-burning spectroscopy, and (4) the results from ab initio calculations.

In principle, the ionization threshold of each molecular species is unique, provided that it can be measured with a high-precision method.[16,17] The IEs of the cis and trans rotamers of HYQ and PDMB were measured by using two-color resonant two-photon ionization (2C−R2PI) spectroscopy.[14] Since this method is subject to the detection of the nonenergy-selected direct ions, it generally leads to an uncertainty of a few tens wavenumbers. Kimura and co-workers have applied 2C−R2PI threshold photoelectron spectroscopy to measure the adiabatic IEs of the two rotational isomers of PDMB in high precision.[18] Recently, Gerhards et al. applied MATI spectroscopy and obtained precise adiabatic IEs of the planar cis and trans rotamers of HYQ.[11] To the best of our knowledge, the vibrational spectra and many other properties of the rotamers of HYQ and PDMB cations are still not available in the literature and need to be explored.

In this paper, we report the threshold ion spectra of the selected rotamers of HYQ and PDMB by using the MATI technique. The selection was done by fixing the frequency of the excitation laser to a particular vibronic transition of the chosen species for successive excitation/ionization. To examine

* Corresponding author. Tel: (886)2-23668236. Fax: (886)2-23620200. E-mail: wbt@sinica.edu.tw.

10.1021/jp0123334 CCC: $20.00
Published on Web 11/30/2001

whether a significant change in molecular geometry during the electronic transition, several vibronic states were used as the intermediate levels for recording the MATI spectra.[19−21] The experimental results yield precise adiabatic IEs of the rotamers and vibrational features of the corresponding cations. They provide information about the relative stabilities of the rotamers in the cationic and neutral ground states, which can be compared with those predicted by ab initio and DFT calculations. We have also performed theoretical calculations to compute the energies of the associated transition state species, leading to the barriers to the rotation of the OH and OCH_3 substitutuents in the S_0, S_1, and cationic ground states. The results, which give the cis-trans isomerization energy, can be used to evaluate the feasibility of the species separation from a chemical sample. In addition, investigations on the frequencies of each mode of different rotamers can reflect the extent of the OH and OCH_3 substitutents involved in the overall vibrations of the cations.

2. Experimental and Computational Details

2.1. Experimental Section. The experiments reported in this paper were performed with a laser-based TOF mass spectrometer as described in our previous publication.[22,23] HYQ (99% purity) and PDMB (99% purity) were purchased from Aldrich Corporation and used without further purification. The solid sample was heated to provide sufficient vapors, seeded into 2 bar of helium, and expanded into the vacuum through a pulsed valve with a 0.15 mm diameter orifice. The molecular beam was collimated by a skimmer located 15 mm downstream from the nozzle orifice. During the experiments, the gas expansion and the ionization regions were maintained at a pressure of about 1×10^{-3} and 1×10^{-5} Pa, respectively.

The two-color resonant two-photon excitation/ionization process was initiated by utilizing two independent tunable UV laser systems controlled by a pulse delay generator (Stanford Research Systems, DG 535). The excitation source is a Nd:YAG pumped dye laser (Quanta-Ray GCR-3/PDL-3; Rhodamin 590, 610, 620, and 640 dyes) with bandwidth ≤ 0.3 cm^{-1}. The visible radiation is frequency doubled to produce UV radiation. The ionization UV laser (Lambda-Physik, ScanmateUV with BBO−III crystal; DCM and LDS 698, 722, and 765 dyes) was pumped by a frequency-doubled Nd:YAG laser (Quantel, Brilliant B). The wavelengths of both dye lasers were calibrated using a Fizeau-type wavemeter (New Focus 7711). The respective UV laser outputs were monitored with two separated photodiodes and fed into a transient digitizer (LeCroy LT224). The two counter-propagating laser beams were focused and intersected perpendicularly with the skimmed molecular beam at 50 mm downstream from the nozzle orifice.

In the MATI experiments, both the prompt ions and the Rydberg neutrals were formed simultaneously in the laser and molecular beam interaction zone. A pulsed electric field of −1 V/cm (duration = 10 μs) was switched on ~0.74 μs after the occurrence of the laser pulses to reject the prompt ions. After a time delay of ~9.60 μs, a second pulsed electric field of +200 V/cm (duration = 10 μs) was applied to field-ionize the Rydberg neutrals. These threshold ions were then accelerated and passed a 1.0 m field-free region before being detected by a dual-stacked microchannel plate particle detector. The ion signal from the detector was collected and analyzed by a multichannel scaler (Stanford Research Systems, SR430). The multichannel scaler and the transient digitizer were interfaced to a personal computer. Mass spectra were accumulated at 1.2 cm^{-1} spacing for 300 laser shots. Composite optical spectra of intensity versus wavelength were then constructed from the individual mass spectra. As the detected ion signal is proportional to the photon intensities of the excitation and ionization lasers for a two-color two-photon process, the obtained optical spectra were normalized to the laser power in order to avoid spurious signals due to shot-to-shot laser fluctuation.

2.2. Computational Section. Ab initio and density functional theory (DFT) calculations were performed using the GAUSSIAN 98 program package.[24] The restricted and unrestricted Hartree−Fock (HF) and DFT methods using various basis sets were performed for predicting the structure parameters, total energies, and vibrational frequencies. The IE was obtained as the difference in the ZPLs of the cation and the corresponding neutral in the ground state. It has been reported that the IE can be computed by using the Gaussian-2 (G-2) and DFT methods to a reasonable accuracy.[25] Although the G-2 calculations may provide more accurate results, they are quite costly for a medium size molecule like PDMB. Therefore, we have performed the HF and DFT calculations with various basis sets for predicting the IEs. It was found that the DFT method yields better results than the HF method. Only the results from the Becke three-parameter functional with the PW91 correlation functional (B3PW91) calculations are presented in this paper. Furthermore, recent advances in computational techniques have enabled us to predict the electronic excitation energy with reasonably good accuracy.[21,26] The time-dependent B3PW91 functional method with the 6-31G** basis set was used to calculate the exited state energy for obtaining the electronic transition energy for these species.

Since the calculations for obtaining fundamental vibrational frequencies are on the basis of the harmonic oscillator model, the obtained values need to be scaled by an appropriate value to correct approximately for the combined errors stemming from basis set incompleteness and neglect of electron correlation and vibrational anharmonicity.[27] The magnitude of the scaling factor depends on (1) the molecular system, (2) the electronic state, (3) the computational method, and (4) the basis set. It was found that the vibrational frequencies at the unrestricted HF/6-31G* calcuations scaled by 0.93 match very well with the experimental values for the two conformers of HYQ in the cationic ground state. In a similar fashion, a scaling factor of 0.95 was found to be suitable for the PDMB cations. To predict the vibrational frequencies of the conformers of HYQ and PDMB in the electronically excited S_1 state, the configuration interaction singles (CIS) method was applied with the 6-31G* basis set. It was found that the calculated values scaled by 0.90 are very close to those obtained from the R2PI experiments.[12,13]

3. Results

3.1. MATI Spectra of HYQ. It has been reported that the vibronic bands of HYQ appear in two series built on 33 535 and 33 500 cm^{-1}, corresponding to the origins of the planar cis and trans rotamers, respectively.[8,12,14,28−29] In general, the signal resulting from the direct ions is more intense than that from the threshold ions.[22] As a common practice, we carry out the 2C−R2PI experiments to locate the ionization threshold of the selected species before applying MATI spectroscopy for recording the threshold ion spectra. Figure 1a−c displays the MATI spectra of *cis*-HYQ recorded by ionizing via the 0^0 vibrationless, $6a^1$ (33969 cm^{-1}), and 1^1 (34355 cm^{-1}) vibrational levels in the S_1 state. Since the MATI technique involves ionization of molecules in high-*n* Rydberg states by a small delayed pulsed field, it results in a sharp peak for the ionization threshold.[30] The leftmost bands in the spectra rise from the transition to form the vibrationless cations. If the uncertainty in the laser

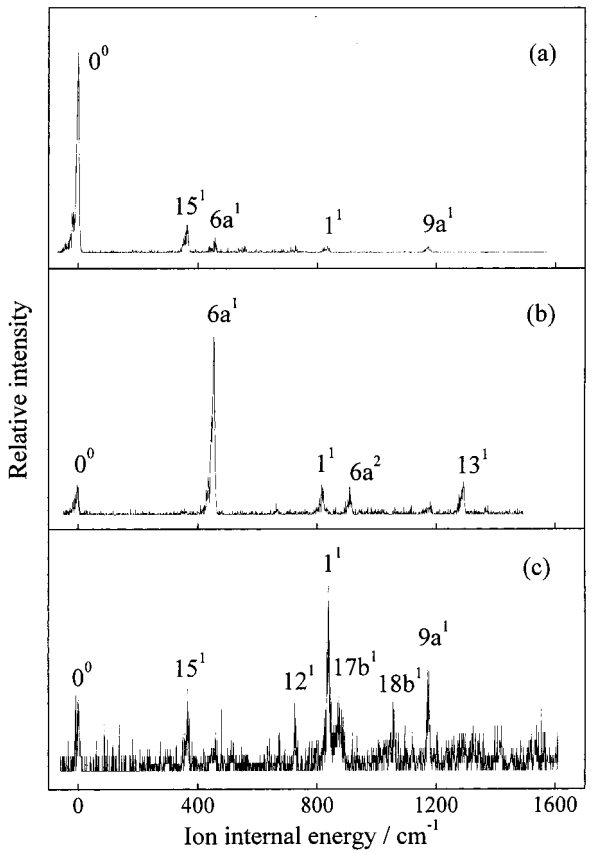

Figure 1. MATI spectra of *cis*-HYQ, recorded by ionizing via the (a) $S_1 0^0$, (b) $S_1 6a^1$, and (c) $S_1 1^1$ intermediate states.

photon energy and the spectral width were taken into account, the field-corrected adiabatic IE of *cis*-HYQ becomes 64051 ± 5 cm^{-1}, which is in excellent agreement with those measured by our 2C−R2PI and the previous MATI experiments.[11] When the $S_1 6a^1$ vibronic state is used as the intermediate level, the band related to mode 6a appears to be the most intense in the MATI spectrum, as seen in Figure 1b. This indicates that the geometry of the cation resembles that of the neutral molecule in the S_1 state.[19−21] A similar finding can be seen when the $S_1 1^1$ vibronic state was used as the intermediate level, as shown in Figure 1c.

The spectral features shifted from the 0^0 band are related to the vibrations of the cations. The observed band intensity in the MATI spectra is related to (1) the oscillator strength corresponding to the $S_1 \leftarrow S_0$ transition, (2) the transition cross section from the S_1 state to the Rydberg state, and (3) the pulsed field ionization efficiency. The assignments to the spectral features were made mainly on the basis of the unrestricted HF/6-31G* calculations and conformity with the experimental data of the corresponding species in the S_0 and S_1 states, as listed in Table 1. The observed MATI bands at 365, 454, 724, 838, 875, 1055, 1174, and 1292 cm^{-1} result from the active vibrations 15^1, $6a^1$, 12^1, 1^1, $17b^1$, $18b^1$, $9a^1$, and 13^1, respectively. It is noted that mode 15 mainly involves in-plane bending C−O vibration with a_1 symmetry is active for the cis but inactive for the trans rotamer. In the contrast, mode 9b that involves in-plane bending C−O vibration with a_g symmetry is active for the trans isomer but inactive for the cis rotamer.

The MATI spectra of *trans*-HYQ recorded by ionizing via the 0^0 vibrationless, $6a^1$ (33935 cm^{-1}), and 1^1 (34321 cm^{-1}) vibrational levels in the S_1 state are shown in Figure 2a−c. The field-corrected adiabatic IE of *trans*-HYQ is found to be

TABLE 1: Observed bands in the MATI Spectra of the Planar cis and trans Rotamers of HYQ and Possible Assignments[a]

cis				trans				
level in S_1 state				level in S_1 state				assignment and approximate description
0^0	$6a^1$	1^1	calcd	0^0	$6a^1$	1^1	calcd	
365		367	367					15^1, βCO
				439			433	$9b^1$, βCO
456	454		460	459	460	458	460	$6a^1$, βCCC
		724	723					12^1, βCCC
834	815	838	836	837		837	837	1^1, breathing
		875	889			882	860	$17b^1$, γCH
	909				905			$6a^2$, βCCC
		1055	1110					$18b^1$, βCH; βOH
1174	1173	1172	1173	1175		1170	1218	$9a^1$, βCH
	1292		1338		1294		1361	13^1, νCO

[a] The experimental values are shifts from 64051 and 63998 cm^{-1} for the planar cis and trans rotamers of HYQ, respectively, whereas the calculated ones (scaled by 0.93) are obtained from the unrestricted HF/6-31G* calculations. ν, β, and γ represent stretching, in-plane bending, and out-of-plane bending vibrations, respectively.

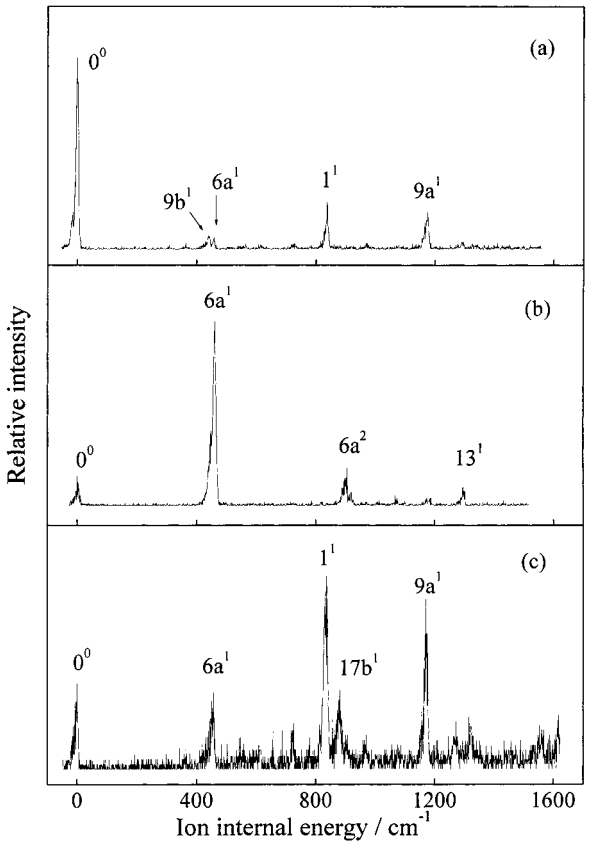

Figure 2. MATI spectra of *trans*-HYQ, recorded by ionizing via the (a) $S_1 0^0$, (b) $S_1 6a^1$, and (c) $S_1 1^1$ intermediate states.

63998 ± 5 cm^{-1}, which is lower than that of *cis*-HYQ by about 53 cm^{-1}. The general spectral features related to the active vibrations of the cations of the two rotamers are quite similar to each other, as seen Figures 1 and 2. The observed vibrations of the *trans*-HYQ cation are listed in Table 1. It is noted that the frequency of each mode slightly differs from each other for the two rotamers. This indicates that the involvement of the hydroxyl group in the overall vibrations of these observed vibrations of the cations is not significant. A similar finding has been reported for the rotamers of resorcinol cations.[11]

3.2. MATI Spectra of PDMB. Similar to the case of HYQ, the vibronic bands of PDMB occur in two series built on 33 852

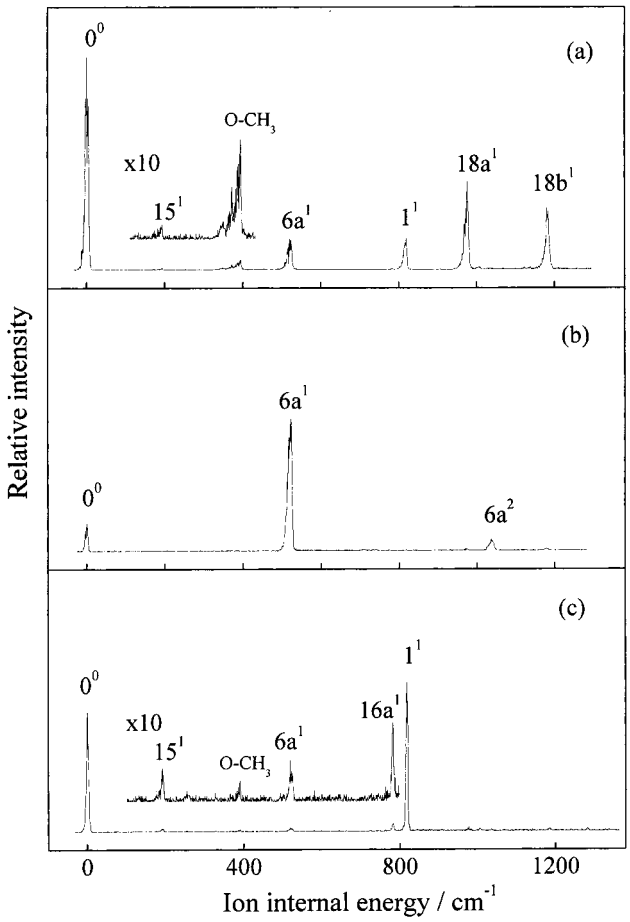

Figure 3. MATI spectra of *cis*-PDMB, recorded by ionizing via the (a) $S_1 0^0$, (b) $S_1 6a^1$, and (c) $S_1 1^1$ intermediate states.

and 33 631 cm^{-1}, corresponding to the origins of the planar cis and trans rotamers, respectively.[9,13−14] Figure 3a−c depicts the MATI spectra of *cis*-PDMB recorded via the 0° vibrationless and $6a^1$ (34 357 cm^{-1}) and 1^1 (34 658 cm^{-1}) vibrational levels in the S_1 state. The adiabatic IE of *cis*-PDMB is determined to be 60772 ± 5 cm^{-1}, which are in good agreement with that measured by the ZEKE experiments as reported in the literature.[18] The vibrational frequencies of the observed MATI bands are listed in Table 2, along with the calculated values and possible assignments. When the vibrationless $S_1 0^0$ state is used as the intermediate level, the active vibrations $6a^1$, 1^1, $18a^1$, and $18b^1$ appear at 523, 819, 977, and 1184 cm^{-1}, respectively, with moderate intensity. The weak bands at 189 and 395 cm^{-1} result from the in-plane bending vibrations C−O and O−CH_3, respectively. Similar active vibrations are observed when the $S_1 6a^1$ and $S_1 1^1$ vibronic levels are used as the intermediate states, as seen in Figure 3b,c.

Figure 4a−c displays the MATI spectra of *trans*-PDMB recorded via the 0° vibrationless and $6a^1$ (34013 cm^{-1}) and 1^1 (34438 cm^{-1}) vibrational levels in the S_1 state. The adiabatic IE of *trans*-PDMB is measured to be 60 563 ± 5 cm^{-1}, which is lower than that of *cis*-PDMB by about 209 cm^{-1}. Analyses on the spectral bands indicate that the observed cation vibrations of the trans rotamer are quite similar to those of the cis rotamer, as listed in Table 2. It is interesting to note that the bands corresponding to mode 6a appear at 396 and 523 cm^{-1} for the trans and cis rotamers, respectively. Figure 5 shows the normal vibration 6a of these species on the basis of the CIS and unrestricted HF methods with the 6-31G* basis set for the S_1 and cationic ground state, respectively. Investigations of the

TABLE 2: Observed Bands in the MATI Spectra of the Planar cis and trans Rotamers of PDMB and Possible Assignments[a]

cis				trans				assignment and approximate description
level in S_1 state				level in S_1 state				
0^0	$6a^1$	1^1	calcd	0^0	$6a^1$	1^1	calcd	
189		192	187					15^1, β(CO)
395		390	373					β(O-CH_3)
523	523	523	529	394	396	395	404	$6a^1$, β(CCC)
				545		540	526	$6b^1$, β(CCC)
		783			789	776		$16a^2$, γ(CCC)
819		818	833	817	817	815	836	1^1, breathing
977		977	935	975			966	$18a^1$, β(CH)
	1039							$6a^2$, β(CCC)
1184		1186	1175	1175		1175	1169	$18b^1$, β(CH)
				1209	1212	1210	1223	$9a^1$, β(CH)

[a] The experimental values are shifts from 60772 and 60563 cm^{-1} for the planar cis and trans rotamers of PDMB, respectively, whereas the calculated ones (scaled by 0.95) are obtained from the unrestricted HF/6-31G* calculations. ν, β, and γ represent stretching, in-plane bending, and out-of-plane bending vibrations, respectively.

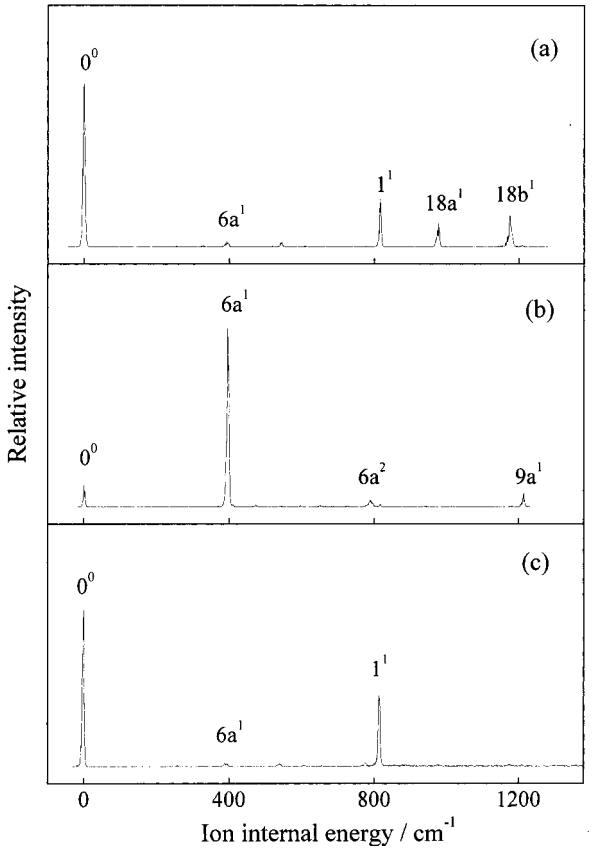

Figure 4. MATI spectra of *trans*-PDMB, recorded by ionizing via the (a) $S_1 0^0$, (b) $S_1 6a^1$, and (c) $S_1 1^1$ intermediate states.

atomic displacements on the basis of ab initio calculations show that mode 6a of the *trans*-PDMB cation involves the in-plane ring deformation and O−CH_3 bending vibrations. Nevertheless, mode 6a of *cis*-PDMB is a nearly pure in-plane ring deformation. It has been reported that the vibrational frequencies of this mode are 382 and 505 cm^{-1} for the trans and cis rotamers in the S_1 state.[13] The vibrational patterns are found to be similar in the S_1 and cationic ground states, as seen in Figure 5.

4. Discussion

4.1 HYQ. The molecular structures of *cis*- and *trans*-HYQ have been determined by Caminati et al.[31] using microwave

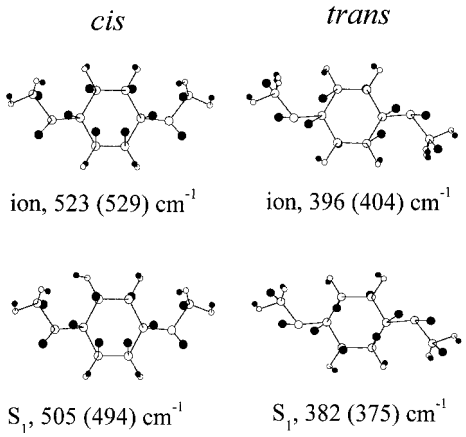

Figure 5. Normal vibration 6a of the cis and trans rotamers of PDMB in the S_1 and cationic ground states on the basis of the CIS/6-31G* and unrestricted HF/6-31G* calculations, respectively. The quoted frequencies are obtained from the R2PI and MATI experiments, whereas the numbers in the parentheses are from the computations.

TABLE 3: Calculated[a] Energies of the Planar cis and trans Rotamers of HYQ in the S_0, and S_1, and Cationic Ground States

	cis	transition state[b]	trans
		S_0 State	
E_R	−382.550971	−382.546184	−382.551112
ZPC	0.109235	0.108384	0.109231
E''	−382.441736	−382.437800	−382.441880
barrier	0.003936	0	0.004080
barrier/cm^{-1}	864	0	895
		S_1 State	
E'	−382.378792	−382.363794	−382.379202
barrier	0.014995	0	0.015405
barrier/cm^{-1}	3291	0	3381
		Ionic State	
E_U	−382.278049	−382.259257	−382.278513
ZPC	0.110462	0.108363	0.110490
E^+	−382.167587	−382.150897	−382.168023
barrier	0.016693	0	0.017129
barrier/cm^{-1}	3664	0	3759
$(E^+ - E'')$/cm^{-1}	60169		60105
exptl IE/cm^{-1}	64051		63998

[a] Calculations are at the restricted B3PW91/6-31G**, time-dependent restricted B3PW91/6-31G**, and unrestricted B3PW91/6-31G** levels for the S_0, S_1, and ionic states, respectively. ZPC is the zero-point correction, and E'' and E^+ are the energies at the zero-point level. 1 Hartree = 27.2116 eV = 219 474.6 cm^{-1}. [b] The H atom of one hydroxyl group is perpendicular to the molecular plane.

spectroscopy. The results show that both of these two rotamers are planar and belong to the symmetry point groups of C_{2v} and C_{2h}, respectively. It has been reported that the structure parameters predicted by both the second-order Møller−Plesset (MP2) and CASSAF calculations are in very good agreement with those of the measured ones.[11,12] We have performed the calculations at the B3PW91/6-31G** level for predicting the relative stabilities and the energy barriers to the OH rotation in the S_0, S_1, and cationic ground states. All calculations show that the trans rotamer lies in a slightly lower energy level than the cis one, as listed in Table 3. In the S_0 state, the zero point level (ZPL) of *trans*-HYQ is lower than that of *cis*-HYQ by 31 cm^{-1}. When the configuration of the transition state is assumed to have the H atom of one of the hydroxyl groups perpendicular to the aromatic ring, the corresponding energy can be calculated with the same procedure. The energy barrier to the rotation of the OH group for the cis−trans isomerization is then estimated to be 864 cm^{-1}, which is slightly less than the lower limit of 1000 cm^{-1} based on the microwave spectroscopic experiments.[31] It has been reported that the energy barrier to the OH rotation in phenol is about 1200 cm^{-1}.[32,33] Thus, the additional OH group in the para position seems to have little effect on the energy barrier for the OH rotation.

The origin of the $S_1 \leftarrow S_0$ electronic transition of *trans*-HYQ is found to be less than that of *cis*-HYQ by 35 cm^{-1}.[8,12,27−28] When taking into account the calculated energies for these species in the ground state, the ZPL in the S_1 state of the trans conformer is expect to lie lower than that of the cis one by 66 cm^{-1}. It has been shown that the later developed time-dependent DFT methods can be used to predict the excited-state energy with a better precision than the CIS procedure for benzene derivatives.[21] The time-dependent B3PW91/6-31G** calculations show that the S_1 state energy of *trans*-HYQ is lower than that of *cis*-HYQ by 90 cm^{-1}. In addition, the energy barrier to the rotation of the OH group for the cis to convert to the trans form in the S_1 state is calculated to be 3291 cm^{-1}, which is much greater than that in the S_0 state. This indicates that the $\pi^* \leftarrow \pi$ transition leads to a stronger interaction between the OH groups and the ring. This argument can be supported by the predicted C−O bond lengths of 1.377, 1.331, and 1.319 Å for both rotamers in the S_0, S_1, and cationic states, respectively, at the MP2/6-31G* level of calculations. The detailed geometry parameters have been reported in previous literature.[12,28]

The adiabatic IEs of the cis and trans rotamers of HYQ have been determined to be 64 051 and 63 998 cm^{-1}, respectively, with the present MATI experiments. When these measured IEs and the calculated energies for the S_0 state are taken into consideration, the ZPL in the cationic ground state of *trans*-HYQ is expected to be lower than that of *cis*-HYQ by 84 cm^{-1}, which is very close to the predicted value of 96 cm^{-1} at the unrestricted B3PW91/6-31G** level. The energy barrier for the cis-trans isomerization is estimated to be 3664 cm^{-1} for the cations. Recently, it has been shown that the investigations on the energy shift in the electronic transition among several deuterium-substituted isotopomers can provide an evidence for the site-specific electronic transition.[17] In the case of aniline, the blue shift in the excitation energy observed for the deuterated species indicates that the $S_1 \leftarrow S_0$ electronic transition mainly takes place around the aromatic ring. In the contrast, the observed red shift in the transition energy to the ionization limit for the deuterated species proves that the transition from the S_1 to the cationic state corresponds to the removal of one of the lone-pair electrons of nitrogen. Similar findings about the energy shifts in the deuterium-substituted systems involving benzene,[34] phenol,[35−37] catechol,[10] and resorcinol[9] have been reported. Therefore, the transition from S_1 to the cationic state is likely to involve the removal of one of the lone-pair electrons of oxygen in HYQ. A relative electron deficiency around the oxygen atom leads to a stronger interaction between the OH groups and the ring for HYQ in the cationic than in the S_1 state. The energy barrier related to the possible cis-trans isomerization of HYQ follows the order $S_0 < S_1 <$ cationic state, as listed in Table 3.

In the present experiments, the HYQ vapors were produced by heating a solid sample to about 100 °C for being seeded in a supersonic expansion. Previous studies show that the planar cis and trans rotamers coexist in the gas phase.[8,11−12,28] As the frequency of the excitation laser is fixed at the well-defined vibronic levels of the selected species for the successive excitation/ionization, only the chosen species is ionized. Since the energy barriers to the OH rotation are relatively high in both the S_1 and cationic states, the cis-trans isomerization is not

TABLE 4: Calculated[a] Energies of the Planar cis and trans Rotamers of PDMB in the S_0, and S_1, and Cationic Ground States

	cis	transition state[b]	trans
		S_0 State	
E_R	−461.128994	−461.124821	−461.128707
ZPC	0.166329	0.165580	0.166222
E''	−460.962665	−460.959241	−460.962485
barrier	0.003424	0	0.003244
barrier/cm^{-1}	751	0	712
		S_1 State	
E'	−460.956636	−460.943526	−460.957235
barrier	0.013110	0	0.013709
barrier/cm^{-1}	2877	0	3009
		Ionic Sate	
E_U	−460.868172	−460.848924	−460.868866
ZPC	0.166711	0.165383	0.166742
E^+	−460.701461	−460.683541	−460.702124
barrier	0.017920	0	0.018583
barrier/cm^{-1}	3933	0	4078
$(E^+ - E'')$/cm^{-1}	57327		57143
exptl IE/cm^{-1}	60772		60563

[a] Calculations are at the restricted B3PW91/6-31G**, time-dependent restricted B3PW91/6-31G**, and unrestricted B3PW91/6-31G** levels for the S_0, S_1, and ionic states, respectively. ZPC is the zero-point correction and E'' and E^+ are the energies at the zero-point level. 1 Hartree = 27.2116 eV = 219 474.6 cm^{-1}. [b] One methyl group is perpendicular to the molecular plane.

expected to occur under the present experimental conditions. Thus, the MATI spectra of the selected rotamer can be precisely recorded.

4.2. PDMB. Previous experimental data and calculated results suggest that several conformers of PDMB may exist in the ground state.[9,13−14,38−39] In addition, only the planar cis and trans forms are stable in the S_1 and cationic ground states. Thus, we only refer to these two structures for the discussion throughout this paper. The B3PW91/6-31G** calculations show that in the S_0 state the ZPL of *cis*-PDMB is lower than that of *trans*-PDMB by 39 cm^{-1} and the energy barrier to the O−CH_3 rotation is 712 cm^{-1}, as listed in Table 4.

The origins of the $S_1 \leftarrow S_0$ electronic transitions are determined to be 33 852 and 33 631 cm^{-1} for the cis and trans rotamers of PDMB, respectively.[9,13−14] This indicates that the ZPL in the S_1 state of the trans lies lower than that of the cis rotamer by 182 cm^{-1}. The time-dependent B3PW91/6-31G** calculations predict that the S_1 state energy of the trans is lower than that of the cis rotamer by 132 cm^{-1} and the energy for the cis-trans isomerization is 2877 cm^{-1}. The higher-energy barrier indicates that the $\pi^* \leftarrow \pi$ transition leads to a stronger interaction between the OCH_3 groups and the aromatic ring for PDMB in the excited S_1 state, as in the case of HYQ.

The difference in the adiabatic IE of the two rotamers of PDMB is found to be 209 cm^{-1}, whereas the discrepancy in the origin of the $S_1 \leftarrow S_0$ electronic transition is 221 cm^{-1}. This indicates that the potential energy surface for the electronic transition from the S_1 to the ionization limit is nearly identical for these two rotamers. The calculated total atomic charges using Mulliken population analysis show that this process mainly involves the removal of one of the lone-pair electrons of oxygen in PDMB. It follows that there is no significant difference in the atomic charge distribution between the cis and trans rotamers of PDMB. When measured IEs and the calculated energies for the S_0 state are taken into consideration, the ZPL in the cationic ground state of *trans*-PDMB is expected to be lower than that of *cis*-PDMB by 170 cm^{-1}, which is very close to the predicted value of 145 cm^{-1} at the B3PW91/6-31G** level. The energy for the cis-trans isomerization for PDMB in the cationic ground state is calculated to be 3933 cm^{-1}, which is greater than those in the S_0 and S_1 states. This indicates that the electron donating CH_3 group enriches the electron density around the oxygen atom of PDMB more in the cationic and the neutral states.

4.3. Vibrations of the Cations of the Rotamers. Ab initio calculations show that the cis and trans rotamers belong to the point groups of C_{2v} and C_{2h}, respectively, for the HYQ and PDMB cations. The spectral features in the MATI spectra of the two conformers are generally similar to each other. However, the frequencies of each mode may slightly differ between the rotamers, resulting from the involvement of the substituent group in the overall vibration. This difference in the vibrational frequency is a measure of the extent of the OH and OCH_3 substitutents involved in the overall molecular motions. Analyses on the MATI spectra of HYQ show that mode 15 corresponding to the in-plane bending C−O vibration with a_1 symmetry is only observed for the cis rotamer whereas mode 9b related to the in-plane C−O bending vibration with a_g symmetry is only seen for the trans rotamer, as shown in Figures 1 and 2. In a similar fashion, mode 15 appears as an active vibration for *cis*-PDMB but not *trans*-PDMB, as seen in Figure 3. The absence of the MATI band corresponding to mode 9b in the MATI spectrum of *trans*-PDMB may result from unfavorable Franck−Condon transition. It is noted that the in-plane O−CH_3 bending vibration is observed for *cis*-PDMB in the cationic state as in the neutral S_1 state. This indicates that the geometry molecular symmetry of the cations resemble those of the neutral species of the two rotamers of PDMB.

In the $S_1 \leftarrow S_0$ electronic transition of HYQ and PDMB, an electron is transferred from the highest occupied molecular orbital (HOMO) to the lowest unoccupied molecular orbital (LUMO).[12,13] This leads to electron redistribution and a stronger interaction between the ring and the OH or OCH_3 group, resulting in a shortening of the C−O bond and a pronounced change of molecular geometry upon electronic excitation. When the vibronic $S_1 6a^1$ state is used as the intermediate level, the MATI bands corresponding to the overtone vibration $6a^2$ of the cations are seen, as shown in Figures 1b, 2b, 3b, and 4b. Since normal vibration 6a mainly involves a ring motion along the long in-plane axis, the decrease in the C−OCH_3 bond length is certainly responsible for the observation of the progression bands. The predicted C−OCH_3 bond lengths are 1.354, 1.328, and 1.291 Å for both rotamers in the S_0, S_1, and cationic states, respectively, at the HF/6-31G* level of calculations.

The observed frequencies of mode 6a for the cis and trans rotamers of the HYQ cations are 454 and 460 cm^{-1}, respectively, as listed in Table 1. Thus, the relative orientation of the two OH groups does not affect the normal vibration significantly. In the contrast, the frequencies of mode 6a for the cis and trans rotamers of PDMB are found to be 523 and 396 cm^{-1}, respectively, as listed in Table 2. This discrepancy in the vibrational frequency results from different extent of the OH group involved in the overall motions. Detailed plots of the atomic displacements on the basis of ab initio calculations show that mode 6a of *trans*-PDMB involves the in-plane ring deformation and the O−CH_3 bending vibrations. Nevertheless, the involvement of OCH_3 group in mode 6a of *cis*-PDMB is not significant. Therefore, investigations on the frequencies of different rotamers can be used as a measure for the extent of the substitutents involved in the overall normal vibration.

5. Conclusion

We have demonstrated that two-color resonant two-photon excitation MATI spectroscopy can be used to probe the ionic

properties of the selected rotamers of HYQ and PDMB. The species selection was achieved by fixing the frequency of the first excitation laser at a particular fingerprint level in the S_1 state of the specific rotamer while tuning the frequency of the second laser across the ionization limit. The adiabatic IEs of *cis*-HYQ, *trans*-HYQ, *cis*-PDMB, and *trans*-PDMB are determined to be 64 051 ± 5, 63 998 ± 5, 60 772 ± 5, 60 563 ± 5 cm^{-1}, respectively. Analyses on the MATI spectra recorded by ionizing via various vibronic states show that the geometries and molecular symmetry in the cationic state resemble those in the S_1 state for these rotamers. The DFT calculations show that the energy barriers related to the possible cis-trans isomerization are relatively high in the S_1 and cationic states. This prediction is in agreement with the observed clean MATI spectra of the selected rotamers with nearly no contributions from the other species.

Analyses on the vibrational features of the cations show that the difference in the vibrational frequency of each mode of different rotamers can reflect the extent of the involvement of the substituent group in the overall normal vibrations. Mode 6a of the cis and trans rotamers of PDMB cations are observed at 523 and 396 cm^{-1}, respectively. Ab initio calculations show that the coupling between the in-plane ring deformation and the $O-CH_3$ bending vibrations is strong in mode 6a of the *trans*-PDMB cation.

Acknowledgment. We gratefully acknowledge the National Science Council of the Republic of China for financial support of this work under Grant Number NSC-90-2113-M-001-038.

References and Notes

(1) Laane, J. *Annu. Rev. Phys. Chem.* **1994**, *45*, 179.
(2) Hollas, J. M. *Chem. Soc. Rev.* **1993**, *22*, 371.
(3) Schlag, E. W.; Neusser, H. J. *Acc. Chem. Res.* **1983**, *16*, 355.
(4) Tzeng, W. B.; Narayanan, K.; Hsieh, C. Y.; Tung, C. C. *J. Chem. Soc., Faraday Trans.* **1997,** *93*, 2981.
(5) Dunn, T. M.; Tembreull, R.; Lubman, D. M. *Chem. Phys. Lett.* **1985**, *121*, 453.
(6) Bürgi, T.; Leutwyler, S. *J. Chem. Phys.* **1994**, *101*, 8418.
(7) Gerhards, M.; Perl, W.; Kleinermanns, K. *Chem. Phys. Lett.* **1995**, *240*, 506.
(8) Patwari, G. N.; Doraiswamy, S.; Wategaonkar, S. *Chem. Phys. Lett.* **1998**, *289*, 8.
(9) Patwari, G. N.; Doraiswamy, S.; Wategaonkar, S. *Chem. Phys. Lett.* **2000**, *316*, 433.
(10) Gerhards, M.; Schumm, S.; Unterberg, C.; Kleinermanns, K. *Chem. Phys. Lett.* **1998**, *294*, 65.
(11) Gerhards, M.; Unterberg, C.; Schumm, S. *J. Chem. Phys.* **1999**, *111*, 7966.
(12) Tzeng, W. B.; Narayanan, K.; Hsieh, C. Y.; Tung, C. C. *Spectrochim. Acta, Part A* **1997**, *53*, 2595 and references therein.
(13) Tzeng, W. B.; Narayanan, K.; Hsieh, C. Y.; Tung, C. C. *J. Mol. Struct.* **1998**, *448*, 91 and references therein.
(14) Oikawa, A.; Abe, H.; Mikami, N.; Ito, M. *Chem. Phys. Lett.* **1985**, *116*, 50.
(15) Yamamoto, S.; Okuyama, K.; Mikami, N.; Ito, M. *Chem. Phys. Lett.* **1986**, *125*, 1.
(16) Shea, D. A.; Goodman, L.; White, M. G. *J. Chem. Phys.* **2000**, *112*, 2762.
(17) Lin, J. L.; Tzeng, W. B. *J. Chem. Phys.* **2001**, *115*, 743.
(18) Cockett, M. C. R.; Okuyama, K.; Kimura, K. *J. Chem. Phys.* **1992**, *97*, 4679.
(19) Lin, J. L.; Tzeng, W. B. *J. Chem. Phys.* **2000**, *113*, 4109.
(20) Huang, L. C. L.; Lin, J. L.; Tzeng, W. B. *Chem. Phys.* **2000**, *261*, 449.
(21) Lin, J. L.; Lin, K. C.; Tzeng, W. B. *Appl. Spectrosc.* **2001**, *55*, 120.
(22) Tzeng, W. B.; Lin, J. L. *J. Phys. Chem. A* **1999**, *103*, 8612.
(23) Lin, J. L.; Tzeng, W. B. *Phys. Chem. Chem. Phys.* **2000**, *2*, 3759.
(24) Frisch, M. J.; Trucks, G. W.; Schlegel, H. B.; Scuseria, G. E.; Robb, M. A.; Cheeseman, J. R.; Zakrzewski, V. G.; Montgomery, J. A., Jr.; Stratmann, R. E.; Burant, J. C.; Dapprich, S.; Millam, J. M.; Daniels, A. D.; Kudin, K. N.; Strain, M. C.; Farkas, O.; Tomasi, J.; Barone, V.; Cossi, M.; Cammi, R.; Mennucci, B.; Pomelli, C.; Adamo, C.; Clifford, S.; Ochterski, J.; Petersson, G. A.; Ayala, P. Y.; Cui, Q.; Morokuma, K.; Malick, D. K.; Rabuck, A. D.; Raghavachari, K.; Foresman, J. B.; Cioslowski, J.; Ortiz, J. V.; Baboul, A. G.; Stefanov, B. B.; Liu, G.; Liashenko, A.; Piskorz, P.; Komaromi, I.; Gomperts, R.; Martin, R. L.; Fox, D. J.; Keith, T,; Al-Laham, M. A.; Peng, C. Y.; Nanayakkara, A.; Gonzalez, C.; Challacombe, M.; Gill. P. M. W.; Johnson, B.; Chen, W.; Wong, M. W.; Andres, J. L.; Gonzalez, C.; Head-Gordon, M.; Replogle, E. S.; Pople, J. A. *Gaussian 98*, Revision A.7; Gaussian, Inc.: Pittsburgh, PA, 1998.
(25) Curtiss, L. A.; Redferm, P. C.; Raghavachari, K.; Pople, J. A. *J. Chem. Phys.* **1998**, *109*, 42.
(26) Casida, M. E.; Jamorski, C.; Casida, K. C.; Salahub, D. R. *J. Chem. Phys.* **1998**, *108*, 4439.
(27) Pople, J. A.; Scott, A. P.; Wong, M. W.; Radom, L. *Isr. J. Chem.* **1993**, *33*, 345.
(28) Humphrey, S. J.; Pratt, D. W. *J. Chem. Phys.* **1993**, *99*, 5078.
(29) Tembreull, R.; Dunn, T. M.; Lubman, D. M. *Spectrochim. Acta, Part A* **1986**, *42*, 899.
(30) Schlag, E. W. *Zeke Spectroscopy*; Cambridge University Press: Cambridge, 1998.
(31) Caminati, W.; Melandri, S.; Favero, L. B. *J. Chem. Phys.* **1994**, *100*, 8569.
(32) Pedersen, T.; Larsen, N. W.; Nygaad, L. *J. Mol. Struct.* **1969**, *4*, 59.
(33) Kim, K.; Jordan, K. D. *Chem. Phys. Lett.* **1994**, *218*, 261.
(34) Neuhauser, R. G.; Siglow, K.; Neusser, H. J. *J. Chem. Phys.* **1997**, *106*, 896.
(35) Bist, H. D.; Brand, J. C. D.; Williams, D. R. *J. Mol. Spectrosc.* **1967**, *24*, 413.
(36) Chewter, L. A.; Sander, M.; Müller-Dethlefs, K,; Schlag, E. W. *J. Chem. Phys.* **1987**, *86*, 4337.
(37) Schütz, M.; Bürgi, T.; Leutwyler, S.; Fischer, T. *J. Chem. Phys.* **1993**, *98*, 3763.
(38) Breen, P. J.; Bernstein, E. R.; Secor, H. V.; Seeman, J. I. *J. Am. Chem. Soc.* **1989**, *111*, 1958.
(39) Anderson, G. M., III; Kollman, P. A.; Domelsmith, L. N.; Houk, K. N. *J. Am. Chem. Soc.* **1979**, *101*, 2344.